TITLE PAGE

Centella asiatica water extract shows low potential for CYP-mediated drug interactions

Kirsten M. Wright, Armando Alcazar Magana, Ronald M. Laethem, Caroline L. Moseley, Troy T. Banks, Claudia S. Maier, Jan F. Stevens, Joseph F. Quinn and Amala Soumyanath

Department of Neurology, Oregon Health and Science University, Portland, Oregon 97239 (KMW, JFQ, AS); Departments of Chemistry (AA, CSM) and Pharmaceutical Sciences (AA, JFS) and Linus Pauling Institute (JFS), Oregon State University, Corvallis, Oregon 97331; BioIVT, Durham, North Carolina 27713 (RML, CLM, TTB), Department of Neurology, Veterans Affairs Portland Health Care System Center, Portland, Oregon (JFQ).

RUNNING TITLE PAGE

CYP mediated drug interaction potential of *Centella asiatica*

Amala Soumyanath, PhD

Associate Professor

Department of Neurology (MC L226)

Oregon Health & Science University

3181 SW Sam Jackson Park Road

Portland, OR 97239

Telephone: 503-494-6878

Fax: 503-494-7358

Email: soumyana@ohsu.edu

Feature	**# words**
Abstract, words	249
Introduction, words	834
Discussion, words	1682
Tables	9
Figures	4

ABBREVIATIONS: ACN, acetonitrile; BLQ, below limits of quantitation; CA, *Centella asiatica*; CAW, *Centella asiatica* aqueous extract; CYP, Cytochrome P450; DMSO, dimethylsulfoxide; FDA, Food and Drug Administration; FOC, fold over control; FLUM, Flumazenil; h, hour(s); HBSS, Hank's Balanced Salts Solution; HDI, herb-drug interaction; HLM, human liver microsomes; HPLC-MS/MS, high performance liquid chromatography- tandem mass

spectrometry; IS, internal standard; KPi, 100 mM potassium phosphate buffer; LC-HRMS, liquid chromatography high-resolution mass spectrometry; LC-HRMS, liquid chromatography- high resolution mass spectrometry; NA, not applicable; NADP, β-Nicotinamide adenine dinucleotide 2′-phosphate; NADPH, β-Nicotinamide adenine dinucleotide 2′-phosphate (reduced form); NC, not calculated; NRS, NADPH regenerating system; min, minute(s); OM, Omeprazole; PAR, peak area ratio; PCR, polymerase chain reaction; PB, phenobarbital; RIF, Rifampicin; RQ, relative quantitation; RT, reverse transcriptase; SCHH, Sandwich-Cultured Human Hepatocytes; TDI, time-dependent inhibition; ThioTEPA, *N*,*N*′,*N*″-Triethylenethiophosphoramide.

ABSTRACT

Centella asiatica (CA) shows considerable promise for development as a botanical drug for cognitive decline. Its primary bioactive components include triterpene glycosides asiaticoside and madecassoside, and their corresponding aglycones asiatic acid and madecassic acid. Exploration of CA's caffeoylquinic acids' bioactivity is ongoing. In this study, an aqueous extract of CA (CAW-R61J) was evaluated for drug interaction potential through inhibition or induction of CYP enzymes, as required by the US Food and Drug Administration. CAW-R61J was assessed for induction potential of CYP1A2, CYP2B6, and CYP3A4 using transporter certified cryopreserved human hepatocytes in sandwich culture. Gene expression of these target CYPs was quantified, and enzyme activities determined to confirm gene expression results. No induction was observed up to 16.7 µg/mL CAW-R61J (equivalent to 1.1 µM asiaticoside 0.8 µM madecassoside, 0.09 µM asiatic acid and 0.12 µM madecassic acid). Reversible and time-dependent inhibitory effects of CAW-R61J on CYP1A2, CYP2B6, CYP2C8, CYP2C9, CYP2C19, CYP2D6 and CYP3A4/5 were evaluated using human liver microsomes. CAW-R61J showed weak reversible inhibition of most of the CYP forms tested; the strongest being of CYP2C9 (IC_{50} of 330 µg/mL). CAW-R61J (≤ 1000 µg/mL) was not a time-dependent inhibitor of any of these CYP enzymes. In summary, CAW-R61J had no, or only a weak impact on CYP induction and inhibition *in vitro*. The clinical relevance of these results will depend on the *in vivo* concentration of CAW-R61J components achieved in humans. Plasma triterpene concentrations measured in our recent clinical studies suggest minimal risk of CYP-mediated drug interactions by these components.

SIGNIFICANCE STATEMENT

A preparation of *Centella asiatica* is currently under clinical development for the prevention or treatment of cognitive decline. The US Food and Drug administration required an evaluation of its potential for drug interactions mediated through drug metabolizing enzymes. This *in vitro* study revealed minimal induction or inhibition of a range of CYP enzymes including CYP3A4 by the *Centella asiatica* extract, suggesting a low potential for drug interactions modulated by CYP metabolism.

INTRODUCTION

Over 80% of the world's population uses botanical medicines (herbal medicines) (Martins, 2013). Many view these medicines as benign because they are of natural origin; however, because their constituents may be metabolized through the same enzymatic pathways as pharmaceutical agents, there is a potential for herb-drug interactions (HDIs). Reported outcomes of such interactions include low drug efficacy, serious toxic reactions to the drug component, and death (Feltrin and Oliveira Simões, 2019; Liu et al., 2019; Maadarani et al., 2019; Martins, 2013; Suroowan and Mahomoodally, 2019). The most important class of enzymes involved in human drug metabolism is cytochrome P450 (CYP) (Savai et al., 2015b), which occurs as a superfamily of related monooxygenase forms responsible for oxidative metabolism of xenobiotics and endogenous compounds (Nebert et al., 2013). The major forms are CYP1A2, CYP2B6, CYP2C8, CYP2C9, CYP2C19, CYP2D6, and CYP3A4/5. Metabolic drug interactions normally occur between two or more drugs such that the addition of the perpetrator drug alters the systemic levels of the victim drug (Bohnert et al., 2016; Lin and Lu, 1998). For example, induction of CYP forms by herbal components, could increase the clearance of the victim drug, thus causing decreased therapeutic efficacy (Shi and Klotz, 2012). Conversely, CYP inhibition by phytochemicals could cause circulating levels of the victim drug to rise to toxic levels (Shi and Klotz, 2012). Investigation of HDIs is undoubtedly a public health priority to ensure the safe use of herbal interventions (Borse et al., 2019).

The US Food and Drug Administration (FDA) has issued guidance for studying metabolic drug interactions *in vitro* using specific tools and methods (FDA, 2020). As the use of herbal healthcare products increases worldwide, it is important to apply the techniques traditionally used for small molecules to determine whether these products have the potential to induce or inhibit CYP forms in humans.

DMD Fast Forward. Published on June 24, 2020 as DOI: 10.1124/dmd.120.090860
This article has not been copyedited and formatted. The final version may differ from this version.

Centella asiatica (L.) Urban (Apiaceae) (CA), commonly known as gotu kola, is a botanical reputed in Eastern medicine to increase intelligence and memory (Kapoor, 1990). Triterpene glycosides, asiaticoside and madecassoside and their corresponding aglycones, asiatic acid and madecassic acid, collectively known as centelloids, are regarded as the predominant bioactive compounds of CA (Brinkhaus et al., 2000), although recent studies by our group suggest a therapeutic role for its caffeoylquinic acid constituents (Gray et al., 2014; Gray et al., 2017b). In preclinical studies, *Centella asiatica* aqueous extract (CAW) demonstrates biological effects of relevance to memory, learning, aging, mood and potentially disease progression in Alzheimer's disease (Gray et al., 2018a; Lokanathan et al., 2016). These include modulation of antioxidant pathways and improved mitochondrial function (Gray et al., 2016; Gray et al., 2018c; Matthews et al., 2019). In addition, similar extracts have been shown to modify brain structure by increasing dendritic arborization of hippocampal neurons (Gray et al. 2018b; Gray et al., 2017b) potentially contributing to the observed cognitive changes.

CA extracts and compounds have been reported to be weak inhibitors of some Phase I drug metabolizing CYP enzymes *in vitro* (Kar et al., 2017; Pan et al., 2010, 2011; Savai et al., 2015a, b; Seeka et al., 2012). In rats, administration of a CA product (composition not provided) increased plasma maximum concentration (14.34%), area under the curve (23%) and elimination half-life (13.81%) of amitriptyline (Khurshid et al., 2018), a substrate of CYP2C19 and CYP2D6 in humans (Mifsud Buhagiar et al., 2019). These studies suggest that CA components may cause drug interactions resulting from altered Phase I metabolism of co-administered drugs.

None of the aforementioned studies investigated the effects on drug metabolizing enzymes of the type of extract (CAW) used in our preclinical studies, and in our current Phase 1 (NCT03929250, NCT03937908) and proposed Phase 2 clinical trials investigating CAW as a botanical drug for cognitive decline. During our application for Investigational New Drug (IND)

status for CAW, the FDA asked us to investigate potential interactions with CYP enzymes. CYP3A4, CYP2D6 and CYP2C19 are of particular interest. The cognitively impaired, elderly target population for CAW may be taking cholinesterase inhibitors donepezil or galantamine, which are substrates for CYP3A4 and CYP2D6 (Coin et al., 2016; Noetzli and Eap, 2013), or drugs for other health conditions, many of which are substrates of CYP3A4 (Zhou et al., 2007).

The composition of plant extracts can vary considerably depending on genetic factors, cultivation conditions and processing methods (Figueiredo, 2017), and this in turn can affect their biological properties. The aim of this study was to assess the specific CAW prepared for use in our clinical trials (CAW-R61J) for its potential to induce or inhibit human forms of CYP.

In the present study, *in vitro* CYP induction potential of CYP1A2, CYP2B6 and CYP3A4 by CAW-R61J was studied using human hepatocytes in sandwich culture (LeCluyse et al., 2000; LeCluyse, 2001). Hepatocytes cultured in this format are responsive to nuclear receptor agonists and maintain important transporter function necessary for proper drug disposition (Yang et al., 2016). Reversible and time-dependent inhibition of CYP forms by CAW-R61J was investigated using standard methods with pooled human liver microsomes (Bohnert et al., 2016; Stresser et al., 2014).

DMD Fast Forward. Published on June 24, 2020 as DOI: 10.1124/dmd.120.090860
This article has not been copyedited and formatted. The final version may differ from this version.

MATERIALS AND METHODS

Materials. Acetaminophen-d_4, azamulin, bupropion hydrocholoride, flumazenil, furafylline, hydroxybupropion-d_6, 4'-hydroxy mephenytoin-d_3, ketoconazole, (S)-mephenytoin, *N*-desethylamodiaquine-d_5, paroxetine hydrochloride, phenacetin, sertraline hydrochloride, N,N',N"-triethylenethiophosphoramide, ticlopidine hydrochloride, and tienilic acid were from Toronto Research Chemicals (North York, ON, Canada). (+)-N-3-Benzylnirvanol, 1'-hydroxymidazolam-d_4, 6β-hydroxytestosterone-d_3, amodiaquin dihydrochloride dihydrate, dextromethorphan hydrobromide monohydrate, dextrorphan-d_3, diclofenac sodium salt, dimethyl sulfoxide, glucose-6-phosphate, glucose-6-phosphate dehydrogenase from baker's yeast (*S. cerevisiae*), Hank's balanced salts solution, magnesium chloride, montelukast sodium, omeprazole, phenelzine sulfate salt, phenobarbital, potassium phosphate monobasic, potassium phosphate dibasic, quinidine, rifampicin, sulfaphenazole, tamoxifen, testosterone, tranylcypromine hydrochloride, and Trypan blue were from Sigma-Aldrich (St. Louis, MO). α-Naphthoflavone and $NADP^+$ were obtained from Cayman Chemicals (Ann Arbor, MI). LC-MS grade acetonitrile, LC-MS grade methanol and formic acid ACS reagent were purchased from Fisher Scientific (Pittsburgh, PA). Imported *Centella asiatica* herb, consisting of dried aerial parts, was purchased from Oregon's Wild Harvest (Redmond, OR, Lots #180700075 and 180600069). Commercial reference phytochemical standards: asiatic acid, asiaticoside, madecassic acid, madecassoside, 5-O-caffeoylquinic acid, 4-O-caffeoylquinic acid, 3-O-caffeoylquinic acid, 1,3-dicaffeoylquinic acid, 1,5-dicaffeoylquinic acid, 3,5-dicaffeoylquinic acid, and quinic acid were purchased from Toronto Research Chemicals (North York, Ontario, Canada); 3,4-dicaffeoylquinic acid, and 4,5-dicaffeoylquinic acid were purchased from Chromadex, (Irvine, CA).

***Centella asiatica* plant material and preparation of CAW-R61J.** Two batches of *Centella asiatica* (Lots #180600069 and 180700075; CA_1 and CA_2 respectively) were purchased for

clinical trial product manufacture. Plant identity was verified by visual inspection, Fourier transform Infra-Red spectroscopy, and thin layer chromatography in comparison with earlier lots of *Centella asiatica* (Gray et al., 2016; Soumyanath et al., 2012), reference standards of characteristic chemical components, and the literature (Bonfill et al., 2006). The material was extracted by Ashland Industries (Kearny, NJ) in two lots (a) 45 kg of CA_1 was boiled under reflux with 562.5 L of water, and (b) 30.5 kg of CA_1 and 14.5 kg of CA_2 were mixed and boiled under reflux with 562.5 L of water. The extracts were cooled to 150°F and pressed through a Sweco 200 Mesh Screen (Florence, KY) to remove plant debris, filtered through filter paper to remove fine debris and then cooled. Aliquots of the two filtrates were shipped to Oregon Health & Science University (OHSU, Portland, OR), where they were frozen and lyophilized, yielding 21.4% from dried CA for CAW-R61F and 23.9% from dried CA for CAW-R61H. The two small scale dried CAWs were mixed in the ratio 4.88 g CAW-R61F to 2.11 g CAW-F61H to yield CAW-R61J. This ratio mimicked that used in the clinical trial product manufacture, which was performed using the major part of the water extracts. Since the chemical composition of CA raw material can vary, we used the specific CAW-R61J extract used to make our clinical trial product in this study.

Voucher samples of the original dried plant materials CA_1 and CA_2 have been deposited at the Oregon State University Herbarium (OSC-V-258630, OSC-V-258631, respectively), while voucher samples of raw plant materials and CAW extracts (CAW-R61F, CAW-R61H and CAW-R61J) are held at OHSU. All dried extract CAW extracts were stored at −20 °C until use.

CAW-R61J fingerprinting. The bioactive centelloids and caffeoylquinic acid compounds in CAW-R61J test material were identified and quantified (MS1 quantification) using LC-HRMS at Oregon State University (OSU; Corvallis, OR) by comparison against co-chromatographed commercial reference standards as previously described (Alcazar-Magana et al., 2020). In addition to [MS1] quantification of known compounds using the area under the curve of the

DMD Fast Forward. Published on June 24, 2020 as DOI: 10.1124/dmd.120.090860
This article has not been copyedited and formatted. The final version may differ from this version.

precursor ion, untargeted LC-HRMS analysis of all the materials was performed. Analytical data on accurate mass (high resolution), isotopic pattern, retention time, and relative peak area of all components detected using both negative and positive electrospray ionization mode were recorded as “fingerprints” of the CAW-R61J extract.

Data-dependent acquisition mode was conducted using a Shimadzu Nexera UPLC system (Columbia, MD) connected to an AB SCIEX TripleTOF® 5600 mass spectrometer (Framingham, MA) equipped with a TurboSpray electrospray ionization source. Chromatographic separation was achieved using an Inertsil Phenyl-3-column (4.6 x 150mm, GL Sciences, Torrance, CA). The injection volume was 10 µL and three technical replicates were carried out. A gradient with solvent A (water containing 0.1% v/v formic acid) and B (methanol containing 0.1% v/v formic acid) was used with a flow rate of 0.4 mL/min in a 35 min chromatographic run. Solvent gradient started at 5% B at 0-1 min, followed by 5-30% B from 1 to 10 min, then 30-100% B from 10-20 min, hold at 100% B from 20-25 min, then return to 5% B from 25-30 min, and then the column was equilibrated with 5% B until 35 min.

Evaluation of CAW centelloid and caffeoylquinic acid stability in cell culture medium alone and in medium from hepatocyte cell cultures. An initial evaluation of stability of centelloids and caffeoylquinic acids present in CAW-R61F (a component of CAW-R61J) in medium alone was performed at OHSU. CAW-R61F (500 µg/mL) was dissolved in cell culture medium, and separate aliquots (1 mL) were placed in a cell culture incubator (37°C, 5% CO_2) or a freezer (-20°C) in sealed containers for 24 h. At the end of this period, triplicate samples (50 µl) from the solutions stored at the two temperatures were prepared for HPLC-MS/MS analysis by addition of ascorbic acid solution (1% w/v; 10 µl) and organic solvent (methanol:acetonitrile, 1:3; 200 µl). Samples were filtered (Ultrafree-UFC 30GVNB 0.22µ spinfilter; Fisher Scientific, Pittsburgh, PA) prior to transfer to HPLC vials.

HPLC-MS/MS of caffeoylquinic acids was performed on an Applied Biosystems Qtrap5500 LC-MS instrument (Framingham, MA). Chromatographic separation was achieved using a Zorbax Eclipse plus C8 rapid resolution column (4.6x150mm, 3.5u, Agilent, Foster City, CA) fitted with a Zorbax Eclipse plus C8 Rapid resolution precolumn (4.6x12.5mm, 5u., Agilent, Foster City, CA). The injection volume was 5 µL. A gradient with solvent A (water, 0.05% acetic acid) and B (acetonitrile, 0.05% acetic acid) was used with a flow rate of 0.8 mL/min in a 21 min run. Solvent gradient increased from 10% to 25% B from 0-4.5 min, to 40% B by 10 min, and to 95% B from 10-11 min. After holding at 95% B from 11-16 min, composition returned to 10% B by 16.2 min and was re-equilibrated at 10% B until 21 min. MS/MS was carried out with electrospray ionization in negative ion mode; transitions monitored were mono-caffeoylquinic acids (353/191) and di-caffeoylquinic acids (515/191). Analysis of the centelloids was performed on an Applied Biosystems Qtrap 4000 LC-MS instrument (Framingham, MA). Chromatographic separation was achieved using a Poroshell 120 EC-C18 column (3 mm id x 50 mm, 2.7µ, Agilent, Foster City, CA) fitted with a Poroshell 120 EC-C18 guard column (3 mm id x 5 mm, 2.7µ, Agilent, Foster City, CA). The injection volume was 20 µL. A gradient with solvent A (water, 10mM ammonium acetate, 0.02% ammonium hydroxide) and B (methanol) was used with a flow rate of 0.42 mL/min in a 9 min run. Solvent gradient increased from 40% B to 60% B from 0-2 min, then increased to 95% B by 3.5 min. After holding at 95% B from 3.5-6 min, the composition returned to 40% B by 6.1 min, and then the column was re-equilibrated with 40% B until 9 min. MS/MS was carried out in in positive ion mode; transitions monitored were Asiatic acid (506/453), madecassic acid (522/451), asiaticoside (976/452), and madecassoside (992/486). Asiatic acid and madecassic acid were monitored as ammonium adducts. For each analyte, the average peak area from triplicate analyses of the solution stored for 24 h at 37 °C was expressed as a % of the average peak area from triplicate analyses of the sample stored for 24 h at -20°C. Caffeoylquinic acid peak area was calculated as total area of all mono-

DMD Fast Forward. Published on June 24, 2020 as DOI: 10.1124/dmd.120.090860
This article has not been copyedited and formatted. The final version may differ from this version.

caffeoylquinic acids or all di-caffeoylquinic acids since we have observed the occurrence of isomerization of these compounds.

Stability of centelloids and caffeoylquinic acids in media from hepatocyte cultures was determined at OSU using the LC-HRMS method described earlier for fingerprinting of CAW-R61J. Compounds of interest were quantified by reference to calibration curves.

Hepatocytes. Human Hepatocyte Culture Transporter Certified™ human hepatocytes were prepared in-house at BioIVT (Baltimore, MD). Three lots of cryopreserved human hepatocytes (Table 1) were thawed rapidly in a 37 °C water bath and transferred to 45 mL of QualGro™ Thaw Medium (BioIVT; Durham, NC) and pelleted at 100×g for 8 min at ambient temperature. The hepatocyte pellet was resuspended in BioIVT QualGro™ Seeding Medium (BioIVT; Durham, NC) and the viability determined using Trypan blue exclusion and a hemocytometer (Fisher Scientific; Pittsburgh, PA). The hepatocytes were diluted to a density of 0.8-1.0 × 10_6 viable cells/mL and seeded (0.5 mL/well) onto Corning® BioCoat® Collagen I 24-well plates (Fisher Scientific; Pittsburgh, PA). The cells were allowed to attach for 18-24 h then overlaid with Hepatocyte Induction Medium supplemented with 0.25 mg/mL Corning® Matrigel® (Fisher Scientific; Pittsburgh, PA) for 18-24 h. After the overlay, the medium was aspirated and cultures treated with compounds. All control compounds were made as 1000× stocks in DMSO and diluted 1:1000 in Hepatocyte Induction Medium. The final concentration of the control compounds was 0.1% DMSO, 25 µM flumazenil (FLUM), 50 µM omeprazole (OM), 1000 µM phenobarbital (PB), or 10 µM rifampicin (RIF). A stock solution of CAW-R61J was made in Hepatocyte Induction Medium at 1 mg/mL and used to make a 50 µg/mL dosing solution. The 50 µg/mL solution was serially diluted (1:3) in Hepatocyte Induction Medium to yield 0.02, 0.07, 0.2, 0.6, 1.9, 5.6, 16.7, or 50 µg/mL. DMSO was added to the CAW-R61J dosing solutions to 0.1% (v/v) such that all treatment conditions contained 0.1% DMSO. All conditions for each donor were carried out in triplicate with treatment every 24 h for a total exposure period of 72 h.

DMD Fast Forward. Published on June 24, 2020 as DOI: 10.1124/dmd.120.090860
This article has not been copyedited and formatted. The final version may differ from this version.

Determination of ATP content in hepatocyte cultures. Cells from donor XVN were cultured as described above. On days 2-4 of culture, hepatocytes were treated in triplicate with culture medium containing positive control (25 µM Tamoxifen), vehicle control (0.1% DMSO), or CAW-R61J (20, 250 or 1000 µg/mL). Following exposure, culture plates were harvested for ATP analysis. Cellular content of ATP was determined using the CellTiter-Glo® Assay Kit provided by Promega (Madison, WI) per manufacturer's instructions. A sample of fresh culture media was included as a no-cell control, and luminescence of all samples was recorded using a Biotek Synergy 4 microplate reader (Winooski, VT).

Determination of CYP mRNA levels in cultured hepatocytes. Following incubation with the CYP probe substrate cocktail, the cultures were washed 2× with 0.5 mL/well HBSS. Cultures were lysed for total RNA isolation by adding 0.2 mL/well of 1:1 mix of Buffer RLT (Qiagen; Waltham, MA) and TRIzol Reagent (ThermoFisher Scientific; Waltham, MA). Plates were sealed and stored frozen at -80 °C until isolation of total RNA. Plates were thawed at ambient temperature. Lysates were thawed and total RNA was isolated from each treatment group using the RNeasy 96 Kit (Qiagen; Waltham, MA) following the manufacturer's instructions. RNA was stored at -80 °C. Isolated RNA was quantified using Quant-iT™ RiboGreen® RNA Assay Kit (ThermoFisher Scientific; Waltham, MA) following manufacturer's instructions. Total RNA (500 ng) was converted to cDNA following the manufacturer's procedure for the High Capacity cDNA Reverse Transcription Kit (Thermo Fisher Scientific; Waltham, MA) on a MiniAmp Plus thermocycler (ThermoFisher Scientific; Waltham, MA). cDNA from human hepatocyte cultures was analysed from each reverse transcription (RT) reaction using the gene-specific TaqMan® assays (ThermoFisher Scientific; Waltham, MA) for CYP1A2, CYP2B6, and CYP3A4. Glyceraldehyde-3-phosphate dehydrogenase (GAPDH) was utilized as an endogenous control for gene expression analysis. Amplifications were performed on a ViiA™ 7 Real-Time PCR System (Thermo Fisher Scientific; Waltham, MA) in relative quantification mode

DMD Fast Forward. Published on June 24, 2020 as DOI: 10.1124/dmd.120.090860
This article has not been copyedited and formatted. The final version may differ from this version.

for 45 amplification cycles using standard conditions for TaqMan®-based assays. Threshold cycle (C_t) determinations were performed by the ViiA™ 7 system software for both target and endogenous control genes. Relative-fold mRNA content was determined for each treatment group relative to the endogenous control gene expression and the calibrator, 0.1% DMSO vehicle control.

Determination of CYP activity in hepatocyte cultures. At the end of the treatment period, CYP1A2, CYP2B6, and CYP3A4/5 activity was determined *in situ* using a method based on Pelletier et al (2013). The treatment medium was aspirated and the cultures washed 2× with 0.5 mL of Hank's Balanced Salts Solution (HBSS) then incubated with 0.3 mL/well HBSS containing a CYP probe substrate cocktail for CYP1A2 (100 µM phenacetin), CYP2B6 (500 µM bupropion), and CYP3A4 (10 µM midazolam). Incubations were performed with shaking on an orbital shaker (150 rpm) at 37 °C for 20 min. Samples of medium were collected and stored at -80 °C until analysed for probe substrate metabolite using LC-MS/MS.

Sample preparation for LC-MS/MS analysis. Internal standard solution (300 µL containing 200 nM d4-acetaminophen, 200 nM d6-hydroxybupropion, and 200 nM d4-1'-hydroxymidazolam in 100% MeOH) was added to each sample (100 µL) in a 96-well deep well plate. After shaking for 15 min, the samples were transferred to a Whatman® 96-well Unifilter® 25 µm MBPP/0.45 µm polypropylene filter plate (Whatman, 7770-0062) stacked on a 96-well deep well plate. Samples were filtered into the deep well plate by centrifugation. The sample filtrate was evaporated to dryness and reconstituted in 150 µL sample diluent (30:70 methanol:5 mM ammonium acetate) and mixed for at least 10 min on a plate shaker. The reconstituted samples were transferred to a Millipore 0.45 µm filter plate (Millipore MSHVN45) and filtered into a Costar 3957 plate by centrifugation. Plates were sealed with a silicone cap mat prior to LC-MS/MS analysis.

LC-MS/MS analysis. LC-MS/MS was conducted using a Thermo Fischer Scientific Vanquish system (Palo Alto, CA) connected to a Thermo Fischer Scientific TSQ Quantis Triple Quadrupole mass spectrometer (Waltham, MA) equipped with an OptaMax NG ionization source and HESI probe. Chromatographic separation was achieved using a Thermo Scientific Hypersil Gold C18 column (50 x 1mm, 1.9 µm; Bellefont, PA). The injection volume was 2 µL and three technical replicates were carried out. A gradient with solvent A (95/5 water/acetonitrile containing 0.2% v/v formic acid) and B (95/5 acetonitrile/water containing 0.2% v/v formic acid) was used with a flow rate of 0.05 mL/min in a 3.5 min chromatographic run. The gradient started at 10% B increasing to 100% B over 1 min, holding at 100% B for 1 min, and then returning to 10% B. Analytes (probe substrate metabolites) and internal standards were detected using electrospray ionization in positive ion mode (Table 2).

Determination of reversible CYP inhibition in HLM. Pooled HLM (*n*= 150, mixed gender, Lot IGF) obtained from BioIVT (Baltimore, MD) were used. Reversible inhibition of CYP forms was determined by carrying out incubations with a constant concentration of CYP probe substrate and increasing concentrations of CAW-R61J in triplicate. Control experiments were carried out in parallel with the probe substrate and increasing concentrations of a control reversible CYP inhibitor in duplicate. The highest concentration of CAW-R61J tested was 1000 µg/mL. A 4× stock solution (4 mg/mL) of CAW-R61J in 100 mM potassium phosphate buffer, pH = 7.4 (KPi) was made and diluted to give a series of 4× stock solutions. These stocks were diluted 1:4 in the reactions to give the final concentrations of CAW-R61J (0, 4, 20, 50, 100, 250, 500, and 1000 µg/mL). Reactions contained HLM (0.1 mg/mL), CAW-R61J or CYP control inhibitor, CYP probe substrate, and an NADPH regenerating system (5 mM glucose-6-phosphate, 1 mM NADP, 5 mM $MgCl_2$, and 1 U/mL glucose-6-phosphate dehydrogenase) in KPi. The reaction components and conditions for each CYP are given in Table 3. Reactions were assembled in round bottom, polypropylene 96 well plates (ThermoFisher Scientific,

Waltham, MA, AB-0796) by adding KPi, HLM, CAW-R61J or control inhibitor, and CYP probe substrate to the wells and equilibrated for 5 min at 37°C. The components of the NADPH regenerating system (NRS) were added together in a separate vessel and equilibrated at 37 °C for 10 min to generate NADPH (~1 mM) before initiating reactions by addition of the charged NRS. The CYP probe substrates used were 60 µM phenacetin for CYP1A2, 80 µM bupropion for CYP2B6, 2 µM amodiaquine for CYP2C8, 5 µM diclofenac for CYP2C9, 80 µM S-mephenytoin for CYP2C19, 5 µM dextromethorphan for CYP2D6, and either 2 µM midazolam or 50 µM testosterone for CYP3A4/5. Reactions were carried out at 37 °C on an orbital shaker (150 rpm) for the times indicated in Table 3. The final organic solvent in all incubations was ≤1% DMSO and ≤0.9% of methanol and/or acetonitrile. A solvent control was carried out for each condition to 100% control activity. All reactions were terminated by the addition of an equal volume of acetonitrile containing stable-labelled internal standard (Table 2). The samples were vortexed and centrifuged for five min to sediment the precipitated protein. Cleared supernatants were transferred to fresh plates and used for the quantitation of the appropriate CYP probe substrate metabolite (Table 2) by LC-MS/MS as described earlier.

Determination of CYP time-dependent inhibition (TDI) in HLM. Lot IGF of HLM was used as above. Potential TDI of CYP enzyme activity by CAW-R61J was determined using the shift in IC_{50} values between 30 min preincubations in the presence and absence of NADPH. Preincubation reactions were assembled in 96 well plates containing HLM (1 mg/mL), CAW-R61J or control, and KPi (Table 9). The reactions were equilibrated for five min at 37 °C before being initiated by the addition of charged NRS or KPi. After 30 min of incubation at 37 °C with shaking at 150 rpm, aliquots of the preincubation reactions were taken and diluted 1:10 in KPi containing the appropriate CYP probe substrate and NRS to measure residual CYP activity (conditions as in Table 3). Both the CAW-R61J dose response reactions and the single concentration TDI control reactions using furafylline (1 μM), thioTEPA (5 μM), phenelzine (100

DMD Fast Forward. Published on June 24, 2020 as DOI: 10.1124/dmd.120.090860
This article has not been copyedited and formatted. The final version may differ from this version.

μM), tienilic acid (1 μM), ticlopidine (10 μM), paroxetine (0.5 μM) and azamulin (0.5 μM) were carried out in triplicate. All reactions were terminated by the addition of an equal volume of acetonitrile containing stable-labelled IS (Table 2). The samples were vortexed and centrifuged for five min to sediment the precipitated protein. Cleared supernatants were transferred to fresh plates and used for the quantitation of the appropriate CYP probe substrate metabolite (Table 2) by LC-MS/MS as described earlier. Unless otherwise specified, all results were expressed as the mean ± standard deviation of triplicate determinations.

CYP mRNA induction data analysis. The C_t values (the fractional cycle number at which the fluorescence passes the fixed threshold) were determined as described above. Each target gene sample was normalized (ΔC_t) by subtracting the C_t for its corresponding endogenous control (GAPDH). In addition, the $\Delta\Delta C_t$ was determined for positive control inducers and the test articles by subtracting the ΔC_t of its corresponding solvent control. Fold changes in target gene expression were determined by taking 2 to the power of the $\Delta\Delta C_t$ ($2^{-\Delta\Delta C_t}$).

For comparison of mRNA responses, the percent of treatment induction response as compared to the positive control induction response were calculated using equation 1 where CYP mRNA FOC_{Sample} is the mRNA fold over control (FOC) value of the CAW-R61J treated samples, CYP mRNA $FOC_{Vehicle}$ is the mRNA FOC value of 0.1% DMSO treated samples, and CYP mRNA $FOC_{Pos\ Con}$ is the mRNA FOC value of positive control treated samples. To signify induction, a threshold of 2-fold over the vehicle control response and at least 20% of the relevant positive control response was used, a threshold proposed by the FDA (FDA, 2020).

$$\%\ \text{Adjusted Pos Control} = \frac{\text{CYP mRNA } FOC_{Sample} - \text{CYP mRNA } FOC_{Vehicle}}{\text{CYP mRNA } FOC_{Pos\ Con} - \text{CYP mRNA } FOC_{Vehicle}} \times 100 \quad (1)$$

Statistical significance was determined ordinary one-way ANOVA and the Bonferroni multiple comparisons test with 0.1% as the control. Differences with *p* values >0.05 were considered significant. To determine the EC_{50} and E_{max} values, the data from concentration-response (FOC values) curves were fitted to a four-parameter sigmoid (Hill) model, according to equation 2.

$$Y=Bottom + (Top-Bottom)/(1+10^{((LogEC_{50}-X)*HillSlope)}) \quad (2)$$

CYP activity induction data analysis. Activity of CYP1A2, CYP2B6 and CYP3A4/5 was determined in pmol/min/10_6 plated hepatocytes. The fold induction over the control was calculated by dividing the activity in the treated sample by the vehicle control activity and multiplying by 100. To determine the % of the positive control, the equation 3 was used where CYP Activity FOC_{Sample} is the activity FOC values of the CAW-R61J treated samples, CYP Activity $FOC_{Vehicle}$ is the activity FOC values of the 0.1% DMSO treated samples, and CYP Activity $FOC_{Pos\ Con}$ is the activity FOC value of positive control treated samples.

$$\%\ \text{Adjusted Pos Control} = \frac{\text{CYP Activity } FOC_{Sample} - \text{CYP Activity } FOC_{Vehicle}}{\text{CYP Activity } FOC_{Pos\ Con} - \text{CYP Activity } FOC_{Vehicle}} \times 100 \quad (3)$$

To signify induction, a threshold of 40% of the positive control response was used, a threshold proposed by (Fahmi et al., 2010).

CYP inhibition data analysis. The peak area ratio (PAR) of probe substrate metabolite to internal standard was determined for all the CYP inhibition samples. The values for the vehicle treated control samples were taken as 100% CYP activity and compared to the treated samples to determine the % CYP activity. The PAR of the treated samples was divided by the PAR of the control and multiplied by 100 to get the % of control activity. To determine the IC_{50} values, the concentration-response (% control value) curves were fitted to a four-parameter sigmoid (Hill) model, according to equation 2 above (substituting $logEC_{50}$ for $logIC_{50}$). The % TDI is the net

time-dependent inhibition and was determined by taking the % inhibition of the positive TDI control in the presence of NADPH during the 30 min preincubation and subtracting the % inhibition of the positive TDI control in the absence of NADPH.

Graph plotting software: All curve-fitting was carried out using Prism 8.0.2 (GraphPad Software, San Diego, CA).

DMD Fast Forward. Published on June 24, 2020 as DOI: 10.1124/dmd.120.090860
This article has not been copyedited and formatted. The final version may differ from this version.

RESULTS

Chemical characterization of CAW-R61J. The composition of CAW-R61J used in this study with respect to characteristic centelloid and caffeoylquinic acid components was determined using precursor ion quantification by LC-HRMS (Table 4). Detailed untargeted LC-HRMS fingerprint of CAW-R61J, recorded using positive and negative electrospray ionization, is available upon request to the corresponding author.

Evaluation of cytotoxicity prior to CYP induction studies. A pilot study was conducted using SCHH to determine the highest non-cytotoxic concentration of CAW-R61J (Lot XVN, Table 1). SCHH were treated with 20, 250, or 1000 µg/mL CAW-R61J for 72 h and ATP levels were measured. The positive control, 25 µM tamoxifen, caused significant deterioration of the cultures and a complete loss of ATP from the cultures (Figure 1). Since there was very little loss of ATP from the cultures with 20 µg/mL CAW-R61J (10%) after 72 h of treatment, 50 µg/mL was chosen as the highest CAW-R61J concentration used in the induction study. We have previously used 50 µg/mL CAW-R61J with no observed cellular stress in studies with neuroblastoma cells and primary neurons (Gray et al., 2014; Gray et al., 2015; Gray et al., 2017a; Gray et al., 2017b). However, there was some cytotoxicity observed with the 50 µg/mL concentration, so the highest concentration shown in the results is 16.7 µg/mL CAW-R61J.

Centelloid and caffeoylquinic acid stability in medium and hepatocyte cell culture. In a preliminary study, CAW-R61F (a component of CAW-R61J) dissolved in culture medium (without cells) was stored for 24 h in an incubator at 37 °C/ 5% CO_2 or in a freezer at -20 °C, prior to HPLC-MS/MS analysis of caffeoylquinic acids and centelloids. Caffeoylquinic acids were detected in the -20 °C sample, but were below the limit of detection after 24 h at 37 °C. The centelloids were easily detectable in samples held at both temperatures. The glycosides asiaticoside and madecassoside demonstrated mild decline (< 5%) over 24 h at 37 °C, while the aglycones asiatic acid and madecassic acid, increased (4% and 21%) after 24 h at 37 °C, likely

DMD Fast Forward. Published on June 24, 2020 as DOI: 10.1124/dmd.120.090860
This article has not been copyedited and formatted. The final version may differ from this version.

due to hydrolysis of the glycosides. Differences in the size of the % change are likely due to their relative abundance in CAW (Table 4).

Samples of the culture media during hepatocyte incubations were taken at 6 and 24 h after the last addition of CAW-R61J, and compared to the original dosing solutions (CAW-R61J 5.6, 16.7 and 50 µg/mL) for the content of some known components using LC-HRMS (Table 5). The mono- and di-caffeoylquinic acids were below the detection limit in the samples from the two lowest doses of CAW-R61J. All of the caffeoylquinic acids were detected in the 50 µg/mL dose of CAW-R61J, but their levels had reduced considerably (>50%) by 6 h. Interestingly, quinic acid levels increased over this time period, possibly derived from hydrolysis of the caffeoylquinic acids. Madecassoside, madecassic acid, asiaticoside, and asiatic acid were easily detectable in the samples at all starting concentrations. The centelloid glycosides madecassoside and asiaticoside showed modest increases over 24 h. By contrast levels of the aglycones madecassic acid, and, particularly asiatic acid declined over 24 h.

Effect of CAW-R61J on mRNA expression in SCHH. Treatment of SCHH with the positive control CYP inducers (10 µM rifampicin, 1000 µM phenobarbital, and 50 µM omeprazole) resulted in significant increases in mRNA levels for the appropriate target gene in every donor (Table 6). The negative control (25 µM flumazenil) did not cause significant induction of any mRNA signal above the vehicle control, indicating a responsive test system (Table 6). Treatment with CAW-R61J (0.02- 50 µg/mL) did not result in the induction of CYP1A2, CYP2B6, or CYP3A4 mRNA with any donor (Figure 2A). For each enzyme, there was a dose-dependent decrease in mRNA signal for all three donors above 0.6 µg/mL CAW-R61J.

Effect of CAW-R61J on enzyme activity. The effect of CAW-R61J on the enzymatic activity levels of CYP1A2, CYP2B6, and CYP3A4 was examined in parallel with the mRNA levels described above. Both mRNA and activity data were gathered from a single well of SCHH. The positive control CYP inducers (50 µM omeprazole, 1000 µM phenobarbital, and 10

DMD Fast Forward. Published on June 24, 2020 as DOI: 10.1124/dmd.120.090860
This article has not been copyedited and formatted. The final version may differ from this version.

µM rifampicin) resulted in significant increases in activity levels for the appropriate target genes with all three donors (Table 7). The negative control (25 µM FLUM) did not cause significant induction of enzyme activity above the vehicle control, indicating a responsive test system (Table 7). CAW-R61J treatment did not result in the induction of CYP1A2, CYP2B6, or CYP3A4 activity in hepatocytes from any donor (Figure 2B). For each enzyme, there was a dose-dependent decrease in activity for all three donors similar to the mRNA results above (Figure 2A).

Cytotoxicity of CAW-R61J during SCHH culture. In photomicrographs of the cultures from all three donors taken every 24 h throughout the study, there were no morphological changes apparent with the 16.7 µg/mL concentration of CAW that would indicate cellular stress (loss of membrane integrity, blebbing, vacuole formation, etc.; not shown). The 50 µg/mL concentration did show signs of cytotoxicity at the latest time point; therefore, the data for this concentration is not included in Figures 2A and 2B.

Evaluation of reversible CYP inhibition. The positive control reversible inhibitors all reduced their respective CYP enzyme activity (Table 8, Figure 3) in a manner consistent with the literature (Emoto et al., 2003; Ring et al., 1996; Suzuki et al., 2002; Thu et al., 2017; VandenBrink et al., 2011; Walsky et al., 2006; Zhao et al., 2012). CAW-R61J was found to be a relatively weak reversible inhibitor for most of the CYPs tested. The strongest reversible inhibition was against CYP2C9 (IC_{50} 330 µg/mL), and least inhibition was against CYP1A2 and CYP2B6 (IC_{50} >1000 µg/mL). Dose response curves are shown in Figure 3 for CYP3A4, CYP2D6 and CYP2C19.

Evaluation of time-dependent CYP inhibition. The positive control time-dependent inhibitors all reduced their respective CYP enzyme activity in an NADPH and time-dependent manner (Table 9) meeting BioIVT's predetermined acceptance criteria for demonstrating that the test system is capable of detecting TDI in HLM. CAW-R61J was not found to be a time-

dependent inhibitor for any of the CYPs tested up to 1000 µg/mL (Table 9). For all CYP forms examined, there was virtually no difference between the dose response curves with or without NADPH (Figure 4). A shift of 1.5-fold in the IC_{50} that is NADPH- and time-dependent is the commonly used threshold to indicate time-dependent inhibition.

DMD Fast Forward. Published on June 24, 2020 as DOI: 10.1124/dmd.120.090860
This article has not been copyedited and formatted. The final version may differ from this version.

DISCUSSION

Following several studies on the inhibitory potential of CA extracts and compounds, this is the first study investigating the effects of the specific type of CA extract (CAW-R61J; a hot water extract) prepared for use in our preclinical, Phase 1 and Phase 2 clinical studies on CYP enzymes. Plant extracts are complex and their composition will vary depending on the source material and extraction method. While the results of this study are specific to CAW-R61J, a range of doses was tested in an effort to encompass the variable levels of water extractable compounds that may occur between this specific extract and other similarly prepared aqueous extracts. CAW-R61J was characterized by LC-HRMS to be able to relate its effects on CYP activity to specific concentrations of known active compounds. Of these, the centelloids have a limited distribution in the plant kingdom, whereas the caffeoylquinic acids are common in numerous plants used in food and beverages. This makes consideration of the effects of the centelloids on CYP induction and inhibition of particular importance.

In our preliminary studies, CAW-R61J did cause some cytotoxicity in the hepatocyte cultures at higher concentrations, which was unexpected based on data from previous neuroblastoma and primary neuron cell culture studies where up to 200 ug/mL of CAW-R61J has been used (Gray et al., 2015; Gray et al., 2017a; Gray et al., 2017b; Soumyanath et al., 2012). Due to this observation, it was decided that for the induction study, 50 µg/mL would be used as the highest concentration. However, due to toxicity observed at this concentration, only the data up to 16.7 µg/ml (the next highest concentration tested) is considered. CAW-R61J, applied at up to 16.7 µg/mL was found not to induce CYP1A2, CYP2B6, or CYP3A4 in SCHH. However, higher concentrations of CAW-R61J within this range did show some mild toxicity, which could explain the dose-dependent decrease in mRNA signal for all three of the forms tested in all three of the donors. It is also possible that these concentrations of CAW-R61J were causing some biochemical changes in the hepatocytes including down-regulation of CYP genes

that were not apparent visually in the photomicrographs. Nevertheless, no induction of the enzymes was observed at the non-toxic or mildly cytotoxic concentrations of the extract tested.

Metabolic stability of the known CA compounds in media and during the induction experiment was examined. While the caffeoylquinic acids were not stable throughout the dosing period, the centelloids were easily detectable and were relatively stable. Caffeoylquinic acids degraded in medium alone over 24 h showing that their loss in SCHH incubations was not due to cellular metabolism alone. It can be noted (Table 5) that 24 h recovery values for the triterpene glycosides exceed 100%. This may have been due to their release from breakdown of larger sugar-containing moieties. The aglycones do reduce in concentration over the 24 h period, potentially due to metabolism since they do not contain chemically labile functional groups. Due to the stability of the centelloids, the relatively unique and suspected main active constituents of CA, it was decided to not carry out additional dosing during each 24 h incubation period. At the end of the last dosing period of 16.7 μg/ml the triterpene glycosides asiaticoside and madecassoside were present at approximately 1.1 μM and 0.8 μM respectively, while the free aglycones asiatic acid and madecassic acid were present at 0.09 μM and 0.12 μM, respectively. Since no induction was observed with CAW-R61J, we conclude that these concentrations of the centelloids do not induce CYP1A2, CYP 2B6, or CYP3A4 in SCHH. Due to their significant loss by 6 h (Table 4), we are unable to properly assess the induction capacity of caffeoylquinic acids. However, since they are ubiquitous in dietary plants, their effects on CYP are less significant than those of the centelloids.

CAW-R61J (≤1000 μg/mL) was not a time-dependent inhibitor of any CYP form tested. However, it did exhibit weak, reversible inhibition of most CYP forms tested, with the greatest inhibition being of CYP2C9 (IC_{50} 330 μg/mL) and least inhibition of CYP1A2 and CYP2B6 (IC_{50} >1000 μg/mL). These results are consistent with previous Phase I metabolic reaction studies where a CA methanolic extract weakly inhibited human CYP3A4 (IC_{50} 226 μg/mL), CYP2D6

(IC_{50} 140 µg/mL), CYP2C9 (IC_{50} 185 µg/mL), and CYP1A2 (IC_{50} 289 µg/mL) (Kar et al., 2017). Similar results were observed with a CA methanolic extract in human liver microsomes (IC_{50} 60-109 µg/mL) (Savai et al., 2015b). Separately, CA was sequentially extracted with hexane, dichloromethane, ethanol and water. In human CYP forms expressed by *E.coli,* the ethanol and dichloromethane extracts showed a higher inhibitory effect on CYP2C19, CYP2C9, CYP2D6, and CYP3A4 (IC_{50} 17-466 µg/mL), compared to the water (IC_{50} 230-615 µg/mL) or hexane (IC_{50} 113-397 µg/mL) extracts (Pan et al., 2010, 2011). This was also observed in human microsomes using methanolic, ethanolic, and hydro-methanolic extracts of CA (IC_{50} 44 - >200 µg/mL) (Savai et al., 2015a, b).

The lower IC_{50} values (more potent inhibition) observed with other (non-aqueous) CA extracts compared to CAW-R61J may be due to species and test system differences, as well as differences in the levels of the CYP inhibitory components. CA ethanolic extracts have higher levels of less polar compounds (like triterpene aglycones and glycosides) than aqueous extracts, which are richer in polar metabolites (like caffeoylquinic acids) (Gray et al., 2018a). The solvents used may have extracted compounds not found in CAW-R61J. This reinforces the need to investigate the specific botanical extract of interest for its CYP inhibitory and induction potential prior to clinical testing.

Purified centelloids are weak inhibitors in human liver microsomes and human CYP forms expressed by *E.coli* of CYP2C19, CYP3A4, CYP2D6 and CYP 2C9. Madecassic and asiatic acids were found to be more potent (IC_{50} 61- >495 µM and IC_{50} 68-139 µM, respectively) than asiaticoside (IC_{50} 1116- >1564 µM) (Pan et al., 2010, 2011; Savai et al., 2015b). This difference in potency has been proposed to be due to varying degrees of lipophilicity and hydrogen bonding between the aglycones and the glycosides (Pan et al., 2010). A standardized CA extract (ECa-223) containing madecassoside (43%) and asiaticoside (39%), inhibited purified CYP3A4, CYP2C19 and CYP2B6 (IC_{50} 211-871 µg/mL; 200-900 µM), but had no effect on

DMD Fast Forward. Published on June 24, 2020 as DOI: 10.1124/dmd.120.090860
This article has not been copyedited and formatted. The final version may differ from this version.

CYP1A2, CYP2C9, CYP2D6, and CYP2E1 (Seeka et al., 2012). Standard inhibitors of these CYP forms have considerably lower IC_{50} values (0.01 to 5.3 µM; Table 8) indicating just how weak these centelloids are as CYP inhibitors.

The observed lowest IC_{50} for CAW-R61J in this study (CYP2C9; 330 ug/mL) is equivalent to 16 µM madecassoside, 22.1 µM asiaticoside, 1.9 µM asiatic acid, and 2.3 µM madecassic acid. These concentrations are well below the IC_{50} values observed when testing the purified centelloids as described above. Thus other components in CAW-R61J must be responsible for, or contribute to, the inhibitory effects on CYP2C9 or the centelloids may act synergistically to inhibit CYP2C9.

It has been suggested that an IC_{50} of less than 100 µg/mL (for extracts) or 100 µM (for active constituents) should be classified as potent inhibition that could lead to undesirable herb-drug interactions (Obach, 2000; Pan et al., 2011). By this measure, CAW-R61J is a not a potent CYP inhibitor, and also showed no evidence of CYP induction. The clinical consequences, if any, of the weak inhibition by CAW-R61J noted in our study will be dependent on the concentrations of inhibitory CAW-R61J components attained in the liver and other CYP containing tissues after oral administration. In a clinical study performed by our group, daily administration of CAST, a product containing mixed centelloids (96 mg asiaticoside, 84 mg madecassic acid, 60 mg asiatic acid), for six months gave steady state plasma levels of 0.5 µM asiatic acid and 0.07 µM madecassic acid (Lou et al., 2018), significantly lower than the lowest IC_{50} values described earlier for the purified compounds (61 µM and 68 µM) (Pan et al., 2010, 2011; Savai et al., 2015b). Based on the centelloid content of CAW-R61J, we expect similar plasma concentrations for these compounds in our clinical studies using this extract. Again, these levels are lower than the concentrations of these compounds found at the lowest IC_{50} of CAW-R61J (CYP2C9; 330 µg/ml). While higher concentrations may be achieved in the liver, the main site of CYP activity or inhibition, this study suggests that the centelloids in CAW-R61J are

DMD Fast Forward. Published on June 24, 2020 as DOI: 10.1124/dmd.120.090860
This article has not been copyedited and formatted. The final version may differ from this version.

unlikely to result in clinically significant induction or inhibition of CYP 450 in humans.

Ultimately, the clinical relevance of the weak CYP inhibition seen in this study will depend on the IC_{50} values of the, as yet unknown, inhibitory CAW-R61J compounds, and their *in vivo* concentration achieved in humans. In making these comparisons, it will be important to consider the unbound fraction (rather than total concentration) of each compound *in vitro* and in plasma. However, based on the results of the present study, it is expected that administration of the proposed doses of CAW-R61J (up to 4 g) would not cause clinically significant CYP induction or inhibition resulting in herb-drug interactions in humans.

Future studies could focus on identifying the CA compounds associated with the weak CYP inhibition seen in the present study, evaluating their IC_{50} values and comparing these with systemic concentrations achieved in humans. Bioassay (CYP inhibition)-guided fractionation could be performed to isolate and identify these molecules. Once identified, these compounds could be excluded from extracts developed for clinical use of CA if their IC_{50} values and human plasma levels suggest a clinically relevant inhibitory potential.

It will also be important to examine possible interactions of CA derivatives with Phase II drug metabolizing enzymes. CA extract (ECa-223) administered orally to male and female rats at 10, 100, and 1000 mg/kg/d for 90 days, did not alter the activity of hepatic Phase II metabolizing enzymes uridine diphosphate glucuronosyltransferase, glutathione S-transferase, and NADPH:quinone oxidoreductase (Seeka et al., 2017). Hepatic sulfotransferase (SULT) activity was not changed in female rats, whereas a previous study had found a decrease in SULT activity in male rats treated with ECa-223 (Seeka et al., 2017). However, no studies were found on the effects of CA derivatives on Phase II drug metabolism in humans or human derived test systems.

AUTHORSHIP CONTRIBUTIONS

Participated in research design: Wright, Magana, Laethem, Banks, Maier, Stevens, Quinn, Soumyanath

Conducted experiments: Wright, Magana, Laethem, Moseley, Banks

Performed data analysis: Magana, Laethem, Moseley, Banks, Wright, Soumyanath

Wrote or contributed to the writing of the manuscript: Wright, Laethem, Banks, Stevens Soumyanath

REFERENCES

Alcazar Magana A, Wright K, Vaswani A, Caruso M, Reed RL, Bailey CF, Nguyen T, Gray NE, Soumyanath A, Quinn J, Stevens JF, and Maier CS (2020) Integration of mass spectral fingerprinting analysis with precursor ion (MS1) quantification for the characterization of botanical extracts: application to extracts of *Centella asiatica* (L.) Urban. *Phytochem Anal* doi: 10.1002/pca.2936.

Bohnert T, Patel A, Templeton I, Chen Y, Lu C, Lai G, Leung L, Tse S, Einolf HJ, Wang YH, Sinz M, Stearns R, Walsky R, Geng W, Sudsakorn S, Moore D, He L, Wahlstrom J, Keirns J, Narayanan R, Lang D, Yang X, and International Consortium for Innovation and Quality in Pharmaceutical Development (IQ) Victim Drug-Drug Interactions Working Group (2016) Evaluation of a New Molecular Entity as a Victim of Metabolic Drug-Drug Interactions-an Industry Perspective. *Drug Metab Dispos* **44:** 1399-1423.

Bonfill M, Mangas S, Cusido RM, Osuna L, Pinol MT, and Palazon J (2006) Identification of triterpenoid compounds of *Centella asiatica* by thin-layer chromatography and mass spectrometry. *Biomed Chromatogr* **20:** 151-153.

Borse SP, Singh DP, and Nivsarkar M (2019) Understanding the relevance of herb-drug interaction studies with special focus on interplays: a prerequisite for integrative medicine. *Porto Biomed J* **4:** e15.

Brinkhaus B, Lindner M, Schuppan D, and Hahn EG (2000) Chemical, pharmacological and clinical profile of the East Asian medical plant *Centella asiatica*. *Phytomedicine* **7:** 427-448.

Coin A, Pamio MV, Alexopoulos C, Granziera S, Groppa F, de Rosa G, Girardi A, Sergi G, Manzato E, and Padrini R (2016) Donepezil plasma concentrations, CYP2D6 and CYP3A4 phenotypes, and cognitive outcome in Alzheimer's disease. *Eur J Clin Pharmacol* **72:** 711-717.

Emoto C, Murase S, Sawada Y, Jones BC, and Iwasaki K (2003) *In vitro* inhibitory effect of 1-aminobenzotriazole on drug oxidations catalyzed by human cytochrome P450 enzymes: a comparison with SKF-525A and ketoconazole. *Drug Metab Pharmacokinet* **18:** 287-295.

Fahmi OA, Kish M, Boldt S, and Obach RS (2010) Cytochrome P450 3A4 mRNA is a more reliable marker than CYP3A4 activity for detecting pregnane X receptor-activated induction of drug-metabolizing enzymes. *Drug Metab Dispos* **38:** 1605-1611.

FDA- US Department of Health and Human Services Food & Drug Administration Center for Drug Evaluation and Research (2020) *In vitro* drug interaction studies — Cytochrome P450 enzyme- and transporter-mediated drug interactions guidance for industry in *FDA Guidance Documents*.

Feltrin C, and Oliveira Simões CM (2019) Reviewing the mechanisms of natural product-drug interactions involving efflux transporters and metabolic enzymes. *Chem Biol Interact* **314:** 108825.

Figueiredo A (2017) Biological properties of essential oils and volatiles: Sources of variability. *Natural Volatiles & Essential Oils* **4:** 1-13.

Gray NE, Harris CJ, Quinn JF, and Soumyanath A (2016) *Centella asiatica* modulates antioxidant and mitochondrial pathways and improves cognitive function in mice. *J Ethnopharmacol* **180:** 78-86.

Gray NE, Magana AA, Lak P, Wright KM, Quinn J, Stevens JF, Maier CS, and Soumyanath A (2018a) C*entella asiatica*: phytochemistry and mechanisms of neuroprotection and cognitive enhancement. *Phytochemistry Reviews* **17:** 161-194.

Gray NE, Morre J, Kelley J, Maier CS, Stevens JF, Quinn JF, and Soumyanath A (2014) Caffeoylquinic acids in *Centella asiatica* protect against amyloid-beta toxicity. *J Alzheimers Dis* **40:** 359-373.

Gray NE, Sampath H, Zweig JA, Quinn JF, and Soumyanath A (2015) *Centella asiatica* Attenuates Amyloid-beta-Induced Oxidative Stress and Mitochondrial Dysfunction. *J Alzheimers Dis* **45:** 933-946.

Gray NE, Zweig JA, Caruso M, Martin MD, Zhu JY, Quinn JF, and Soumyanath A (2018b) *Centella asiatica* increases hippocampal synaptic density and improves memory and executive function in aged mice. *Brain Behav* **8:** e01024.

Gray NE, Zweig JA, Caruso M, Zhu JY, Wright KM, Quinn JF, and Soumyanath A (2018c) *Centella asiatica* attenuates hippocampal mitochondrial dysfunction and improves memory and executive function in β-amyloid overexpressing mice. *Mol Cell Neurosci* **93:** 1-9.

Gray NE, Zweig JA, Matthews DG, Caruso M, Quinn JF, and Soumyanath A (2017a) *Centella asiatica* Attenuates Mitochondrial Dysfunction and Oxidative Stress in Aβ-Exposed Hippocampal Neurons. *Oxid Med Cell Longev* **2017:** 7023091.

Gray NE, Zweig JA, Murchison C, Caruso M, Matthews DG, Kawamoto C, Harris CJ, Quinn JF, and Soumyanath A (2017b) *Centella asiatica* attenuates Aβ-induced neurodegenerative spine loss and dendritic simplification. *Neurosci Lett* **646:** 24-29.

Kapoor L (1990) Handbook of Ayurvedic Medicinal Plants, CRC Press, Boca Raton, Florida.

Kar A, Pandit S, Mukherjee K, Bahadur S, and Mukherjee PK (2017) Safety assessment of selected medicinal food plants used in Ayurveda through CYP450 enzyme inhibition study. *J Sci Food Agric* **97:** 333-340.

Khurshid F, Govidasamy J, Khalilullah H, Nomani M, Shahid M, Ain M, and Alsultan M (2018) Effect of *Centella asiatica* formulation on the pharmacokinetics of amitriptyline in rats: A herb-drug interaction study. *Latin American Journal of Pharmacy* **37:** 663-670.

LeCluyse E, Madan A, Hamilton G, Carroll K, DeHaan R, and Parkinson A (2000) Expression and regulation of cytochrome P450 enzymes in primary cultures of human hepatocytes. *J Biochem Mol Toxicol* **14:** 177-188.

LeCluyse EL (2001) Human hepatocyte culture systems for the in vitro evaluation of cytochrome P450 expression and regulation. *Eur J Pharm Sci* **13:** 343-368.

Lin JH, and Lu AY (1998) Inhibition and induction of cytochrome P450 and the clinical implications. *Clin Pharmacokinet* **35:** 361-390.

Liu D, Zhang L, Duan LX, Wu JJ, Hu M, Liu ZQ, and Wang CY (2019) Potential of herb-drug / herb interactions between substrates and inhibitors of UGTs derived from herbal medicines. *Pharmacol Res* **150:** 104510.

Lokanathan Y, Omar N, Ahmad Puzi NN, Saim A, and Hj Idrus R (2016) Recent updates in neuroprotective and neuroregenerative potential of *Centella asiatica*. *Malays J Med Sci* **23:** 4-14.

Lou JS, Dimitrova DM, Murchison C, Arnold GC, Belding H, Seifer N, Le N, Andrea SB, Gray NE, Wright KM*,* Caruso M, and Soumyanath A (2018) *Centella asiatica* triterpenes for diabetic neuropathy: a randomized, double-blind, placebo-controlled, pilot clinical study. *Esper Dermatol* **20:** 12-22.

Maadarani O, Bitar Z, and Mohsen M (2019) Adding herbal products to direct-acting oral anticoagulants can be fatal. *Eur J Case Rep Intern Med* **6:** 001190.

Martins E (2013) The growing use of herbal medicines: issues relating to adverse reactions and challenges in monitoring safety. *Front Pharmacol* 177.

Matthews DG, Caruso M, Murchison CF, Zhu JY, Wright KM, Harris CJ, Gray NE, Quinn JF, and Soumyanath A (2019) *Centella asiatica* improves memory and promotes antioxidative signaling in 5XFAD mice. *Antioxidants (Basel)* doi: 10.3390/antiox8120630.

Mifsud Buhagiar L, Sammut C, Chircop Y, Axisa K, Sammut Bartolo N, Vella Szijj J, Serracino Inglot, A, and LaFerla G (2019) Practical liquid chromatography-tandem mass spectrometry method for the simultaneous quantification of amitriptyline, nortriptyline and their hydroxy metabolites in human serum. *Biomed Chromatogr* **33:** e4679.

Nebert DW, Wikvall K, and Miller WL (2013) Human cytochromes P450 in health and disease. *Philos Trans R Soc Lond B Biol Sci* **368:** 20120431.

Noetzli M, and Eap CB (2013) Pharmacodynamic, pharmacokinetic and pharmacogenetic aspects of drugs used in the treatment of Alzheimer's disease. *Clin Pharmacokinet* **52:** 225-241.

Obach RS (2000) Inhibition of human cytochrome P450 enzymes by constituents of St. John's Wort, an herbal preparation used in the treatment of depression. *J Pharmacol Exp Ther* ***294*:** 88-95.

Pan Y, Abd-Rashid BA, Ismail Z, Ismail R, Mak JW, Pook PC, Er HM, and Ong CE (2010) *In vitro* modulatory effects on three major human cytochrome P450 enzymes by multiple active constituents and extracts of *Centella asiatica*. *J Ethnopharmacol* **130:** 275-283.

Pan Y, Abd-Rashid BA, Ismail Z, Ismail R, Mak JW, Pook PC, Er HM, and Ong CE (2011*) In vitro* modulatory effects of *Andrographis paniculata, Centella asiatica* and *Orthosiphon stamineus* on cytochrome P450 2C19 (CYP2C19). *J Ethnopharmacol* **133:** 881-887.

Pelletier RD, Lai WG, and Wong YN (2013) Application of a substrate cocktail approach in the assessment of Cytochrome P450 induction using cultured human hepatocytes. *J Biomol Screen* **18:** 199–210.

Ring BJ, Binkley SN, Vandenbranden M, and Wrighton SA (1996) *In vitro* interaction of the antipsychotic agent olanzapine with human cytochromes P450 CYP2C9, CYP2C19, CYP2D6 and CYP3A. *Br J Clin Pharmacol* **41:** 181-186.

Savai J, Varghese A, Pandita N, and Chintamaneni M (2015a) *In vitro* assessment of CYP1A2 and 2C9 inhibition potential of *Withania somnifera* and *Centella asiatica* in human liver microsomes. *Drug Metab Pers Ther* **30:** 137-141.

Savai J, Varghese A, Pandita N, and Chintamaneni M (2015b) Investigation of CYP3A4 and CYP2D6 interactions of *Withania somnifera* and *Centella asiatica* in human liver microsomes. *Phytother Res* **29:** 785-790.

Seeka P, Niwattisaiwong N, Tantisira MH, Chevapat S, Anuntawuttikul K, Apipalakul K, and Lawanprasert S (2017) Effects of the standardized extract of C*entella asiatica* ECa233 on hepatic Phase II drug-metabolizing enzymes in rats. *Thai J of Pharma Sci* **41:** 41-46.

Seeka P, Niwattisaiwong N, Warisnoicharoen W, Winitthana T, Tantisira M, and Lawanprasert S (2012) Effects of the standardized extract of *Centella asiatica* ECa233 on human cytochrome P450. *Thai Jl of Pharma Sci* **36:**30-37.

Shi S, and Klotz U (2012) Drug interactions with herbal medicines. *Clin Pharmacokinet* **51:** 77-104.

Soumyanath A, Zhong YP, Henson E, Wadsworth T, Bishop J, Gold BG, and Quinn JF (2012) *Centella asiatica* extract improves behavioral deficits in a mouse model of Alzheimer's Disease: Investigation of a possible mechanism of action. *Int J Alzheimers Dis* **2012:** 381974.

Stresser DM, Mao J, Kenny JR, Jones BC, and Grime K (2014) Exploring concepts of in vitro time-dependent CYP inhibition assays. *Expert Opin Drug Metab Toxicol* **10:** 157-174.

Suroowan S, and Mahomoodally MF (2019) Herbal medicine of the 21st century: A focus on the chemistry, pharmacokinetics and toxicity of five widely advocated phytotherapies. *Curr Top Med Chem* **19:** 2718-2738.

Suzuki H, Kneller MB, Haining RL, Trager WF, and Rettie AE (2002) (+)-N-3-Benzyl-nirvanol and (-)-N-3-benzyl-phenobarbital: new potent and selective in vitro inhibitors of CYP2C19. *Drug Metab Dispos* **30:** 235-239.

Thu OKF, Spigset O, and Hellum B (2017) Noncompetitive inhibition of human CYP2C9 in vitro by a commercial *Rhodiola rosea* product. *Pharmacol Res Perspect* doi: 10.1002/prp2.324.

VandenBrink BM, Foti RS, Rock DA, Wienkers LC, and Wahlstrom JL (2011) Evaluation of CYP2C8 inhibition *in vitro*: utility of montelukast as a selective CYP2C8 probe substrate. *Drug Metab Dispos* **39:** 1546-1554.

Walsky RL, Astuccio AV, and Obach RS (2006) Evaluation of 227 drugs for *in vitro* inhibition of cytochrome P450 2B6. *J Clin Pharmacol* **46:** 1426-1438.

Yang K, Guo C, Woodhead JL, St Claire RL, Watkins PB, Siler SQ, Howell BA, and Brouwer KLR (2016) Sandwich-cultured hepatocytes as a tool to study drug disposition and drug-induced liver injury. *J Pharm Sci* **105:** 443-459.

Zhao Y, Hellum BH, Liang A, and Nilsen OG (2012) The *in vitro* inhibition of human CYP1A2, CYP2D6 and CYP3A4 by tetrahydropalmatine, neferine and berberine. *Phytother Res* **26:** 277-283.

Zhou SF, Xue CC, Yu XQ, Li C, and Wang G (2007) Clinically important drug interactions potentially involving mechanism-based inhibition of cytochrome P450 3A4 and the role of therapeutic drug monitoring. *Ther Drug Monit* **29:** 687-710.

FOOTNOTES

This study was supported by the National Institutes of Health, National Center for Complementary and Integrative Health (NCCIH) [Grants R61AT009628, T32AT002688, KL2TR002370-03S1], National Institutes of Health, National Institute on Aging (NIA) [P30 AG008017], and National Center for Research Resources (NCRR) [Grant S10RR027878].

LEGENDS FOR FIGURES

Figure 1. Relative ATP content of SCHH from donor XVN treated with DMSO, tamoxifen, or CAW-R61J. SCHH were treated for 72 h with 0.1% DMSO, 25 μM tamoxifen (TAM), or the indicated concentrations of CAW-R61J. ATP Levels were measured and normalized to the ATP content in the 0.1% DMSO vehicle control. *** $p<0.001$; n=3 per treatment.

Figure 2. Dose–response of CYP mRNA and activity following treatment with CAW-R61J. Fold change of CYP mRNA (A) or CYP activity (B) is plotted relative to the vehicle control (0.1% DMSO) following treatment with CAW-R61J for 72 h. Data shown are the mean and standard error of a triplicate determination in three individual hepatocyte donors. ●Donor XVN, ■Donor IWM, ▲Donor BXW. # - n=2 for Donor XVN. Data from the 50 μg/mL condition is not shown due to cytotoxicity being observed at this concentration.

Figure 3. Reversible inhibition of CYP activity by CAW-R61J in HLM. Data is shown for CYP2C19 (●), CYP2D6 (■), CYP3A4 using midazolam (MDZ) as substrate (▲), and CYP3A4 using testosterone (TST) as substrate (♦). Data shown are the mean ± standard deviation of triplicate determinations.

Figure 4. Time-dependent inhibition (TDI) of CYP2C19 (A), CYP2D6 (B), CYP3A4 using midazolam as substrate (C), and CYP3A4 using testosterone as substrate (D) activity by CAW-R61J in HLM. Potential TDI of CYP enzyme activity by CAW-R61J was determined using the shift in IC_{50} values between 30 min preincubations in the presence and absence of NADPH. All

reactions were performed in triplicate. Data shown are the mean ± standard deviation of triplicate determinations.

DMD Fast Forward. Published on June 24, 2020 as DOI: 10.1124/dmd.120.090860
This article has not been copyedited and formatted. The final version may differ from this version.

TABLES

TABLE 1. Donor demographics for hepatocytes used in the study

Donor	Age	Gender	Race	Viability (%)
XVN	57	M	Caucasian	93
IWM	46	M	Caucasian	93
BXW	73	F	Caucasian	90

DMD Fast Forward. Published on June 24, 2020 as DOI: 10.1124/dmd.120.090860
This article has not been copyedited and formatted. The final version may differ from this version.

TABLE 2. Summary of CYP probe substrate metabolite analysis by LC-MS/MS

Enzyme	Substrate	Metabolite (transition monitored)	Internal Standard (transition monitored)	Internal Standard Concentration[1]
CYP1A2	Phenacetin	Acetaminophen (152→110)	Acetaminophen-d_4 (156→114)	500 nM
CYP2B6	Bupropion	Hydroxybupropion (256→238)	Hydroxybupropion-d_6 (262→244)	100 nM
CYP2C8	Amodiaquine	*N*-Desethylamodiaquine 328→282)	*N*-Desethylamodiaquine-d_5 (333→282)	100 nM
CYP2C9	Diclofenac	4′-Hydroxydiclofenac (312→231)	4′-Hydroxydiclofenac-d4 (316→234)	500 nM
CYP2C19	*S*-Mephenytoin	4′-Hydroxymephenytoin (235→150)	4′-Hydroxymephenytoin-d_3 (238→150)	100 nM
CYP2D6	Dextromethorphan	Dextrorphan (258→157)	Dextrorphan-d3 (261→157)	150 nM
CYP3A4/5	Midazolam	1′-Hydroxymidazolam (342→324)	1′-Hydroxymidazolam-d_4 (346→328)	5 nM
CYP3A4/5	Testosterone	6’-hydroxytestosterone (305→269)	6’-hydroxytestosterone-d3 308→272)	250 ng/mL

[1] Concentration in internal standard solution added to CYP inhibition samples.

DMD Fast Forward. Published on June 24, 2020 as DOI: 10.1124/dmd.120.090860
This article has not been copyedited and formatted. The final version may differ from this version.

TABLE 3. Assay conditions used to measure microsomal CYP enzyme activity and inhibition

Enzyme	Substrate	Substrate Concentration (μM)	Incubation Time (min)	Type of Inhibitor	Positive Control Inhibitor
CYP1A2	Phenacetin	60	10	Reversible	α-Naphthoflavone
				TDI	Furafylline
CYP2B6	Bupropion	80	15	Reversible	Sertraline
				TDI	*N*,*N*′,*N*″-Triethylenethiophosphoramide (ThioTEPA)
CYP2C8	Amodiaquine	2	10	Reversible	Montelukast
				TDI	Phenelzine
CYP2C9	Diclofenac	5	15	Reversible	Sulfphenazole
				TDI	Tienilic acid
CYP2C19	*S*-Mephenytoin	80	25	Reversible	Benzylnirvanol
				TDI	Ticlopidine
CYP2D6	Dextromethorphan	5	10	Reversible	Quinidine
				TDI	Paroxetine
CYP3A4/5	Midazolam	2	5	Reversible	Ketoconazole
				TDI	Azamulin
	Testosterone	50	10	Reversible	Ketoconazole
				TDI	Azamulin

TDI- Time dependent inhibition

TABLE 4. CAW-R61J composition

Compound	Amount of compound (mg/g dry extract)
Asiaticoside	64.13 ± 0.78
Madecassoside	47.26 ± 6.22
Asiatic Acid	2.75 ± 0.02
Madecassic Acid	3.49 ± 0.26
5-O-Caffeoylquinic Acid	1.47 ± 0.01
4-O-Caffeoylquinic Acid	0.54 ± 0.01
3-O-Caffeoylquinic Acid	2.21 ± 0.08
1,5-Dicaffeoylquinic Acid	0.40 ± 0.01
1,3-Dicaffeoylquinic Acid	0.50 ± 0.01
3,4-Dicaffeoylquinic Acid	1.19 ± 0.04
3,5-Dicaffeoylquinic Acid	1.05 ± 0.01
4,5-Dicaffeoylquinic Acid	1.25 ± 0.03

DMD Fast Forward. Published on June 24, 2020 as DOI: 10.1124/dmd.120.090860
This article has not been copyedited and formatted. The final version may differ from this version.

TABLE 5. Metabolic stability of CAW-R61J components during the final 24-h of treatment

Compound	5.6 µg/mL CAW-R61J			16.7 µg/mL CAW-R61J			50 µg/mL CAW-R61J		
	Time 0	% of Time 0		Time 0	% of Time 0		Time 0	% of Time 0	
	Amount of Compound (ng/mL)	6 h	24 h	Amount of Compound (ng/mL)	6 h	24 h	Amount of Compound (ng/mL)	6 h	24 h
5-O-Caffeoylquinic Acid	0.7 ± 0.1	70	0	4 ± 1	92	0	9 ± 1	46	32
4-O-Caffeoylquinic Acid	BLQ	BLQ	BLQ	BLQ	BLQ	BLQ	20 ± 1	0	0
3-O-Caffeoylquinic Acid	BLQ	BLQ	BLQ	BLQ	BLQ	BLQ	13 ± 1	0	0
1,5-Dicaffeoylquinic Acid	BLQ	BLQ	BLQ	0.9 ± 0.1	0	0	3.8 ± 0.1	30	0
1,3-Dicaffeoylquinic Acid	BLQ	BLQ	BLQ	0.7 ± 0.1	0	0	3.7 ± 0.1	29	28
3,4-Dicaffeoylquinic Acid	4 ± 1	0	0	11 ± 1	BLQ	BLQ	41 ± 5	31	21
3,5-Dicaffeoylquinic Acid	BLQ	BLQ	BLQ	BLQ	BLQ	BLQ	17 ± 1	0	0
4,5-Dicaffeoylquinic Acid	BLQ	BLQ	BLQ	BLQ	BLQ	BLQ	28 ± 2	0	0
Quinic Acid	38 ± 2	101	149	102 ± 4	106	153	303 ± 10	95	131
Madecassoside	155 ± 3	100	121	367 ± 44	125	145	1222 ± 129	104	116
Asiaticoside	123 ± 18	97	113	383 ± 38	113	130	1402 ± 152	92	101
Asiatic Acid	17 ± 3	81	63	27 ± 2	76	41	69 ± 3	65	19
Madecassic Acid	11 ± 2	76	54	43 ± 1	80	60	136 ± 6	91	88

BLQ- Below the Limit of Quantitation.

TABLE 6. Induction of CYP mRNA in SCHH after treatment for 72 h with DMSO, flumazenil, omeprazole, phenobarbital, or rifampicin.

CYP	Concentration	XVN				IWM				BXW			
		Fold over vehicle control		% positive control		Fold over vehicle control		% positive control		Fold over vehicle control		% positive control	
		Mean	SD	Mean	SD	Mean	SD	Mean	SD	Mean	SD	Mean	SD
1A2	0.1% DMSO	1.3	0.89	0.0	1.2	1.5	1.6	0.0	24	1.0	0.046	0.0	0.18
	25 µM Flumazenil	3.8	NA	3.3	NA	0.91	0.080	-8.6	1.2	1.8	0.59	3.0	2.3
	50 µM Omeprazole	77***	NA	100	NA	8.2***	1.8	100	27	26***	1.8	100	7.0
2B6	0.1% DMSO	1.0	0.045	0.0	0.41	1.0	0.037	0.0	0.16	1.1	0.41	0.0	2.8
	25 µM Flumazenil	1.4	0.11	3.4	0.99	1.7	0.16	3.2	0.73	1.9	0.38	6.0	2.6
	1000 µM Phenobarbital	12***	1.3	100	11	23***	7.6	100	34	16***	2.7	100	18
3A4	0.1% DMSO	1.0	0.18	0.0	0.46	1.0	0.045	0.0	0.18	1.0	0.20	0.0	1.4
	25 µM Flumazenil	1.7	0.26	1.9	0.67	1.2	0.065	0.93	0.26	2.0	0.25	6.7	1.7
	10 µM Rifampicin	40***	4.9	100	12***	26	4.8	100	19	16***	0.40	100	2.7

***P<0.0001; NA- Not applicable; n=2.

TABLE 7. Induction of CYP activity in SCHH after treatment for 72 h with DMSO, flumazenil, omeprazole, phenobarbital, or rifampicin.

CYP	Concentration	XVN				IWM				BXW			
		Fold over vehicle control		% positive control		Fold over vehicle control		% positive control		Fold over vehicle control		% positive control	
		Mean	SD	Mean	SD	Mean	SD	Mean	SD	Mean	SD	Mean	SD
1A2	0.1% DMSO	1.0	0.087	0.0	0.41	1.0	0.13	0.0	0.91	1.0	0.051	0.0	0.38
	25 µM Flumazenil	1.4	0.21	2.0	1.0	1.3	0.13	2.4	0.91	1.5	0.62	3.5	4.6
	50 µM Omeprazole	22***	2.1	100	9.7	15***	1.4	100	10	14***	1.8	100	14
2B6	0.1% DMSO	1.0	0.082	0.0	2.0	1.0	0.069	0.0	2.9	1.0	0.11	0.0	3.3
	25 µM Flumazenil	1.0	0.083	0.99	2.0	1.1	0.090	4.0	3.8	1.2	0.092	6.4	2.8
	1000 µM Phenobarbital	5.1***	0.44	100	11	3.4***	0.49	100	21	4.3***	0.17	100	5.3
3A4	0.1% DMSO	1.0	0.036	0.0	0.46	1.0	0.070	0.0	0.90	1.0	0.45	0.0	10
	25 µM Flumazenil	1.1	0.095	1.1	1.2	1.1	0.10	1.2	1.3	0.92	0.28	-1.8	6.4
	10 µM Rifampicin	8.8***	0.49	100	6.3	8.8***	0.22	100	2.8	5.3***	1.8	100	42

***P<0.0001.

DMD Fast Forward. Published on June 24, 2020 as DOI: 10.1124/dmd.120.090860
This article has not been copyedited and formatted. The final version may differ from this version.

TABLE 8. Reversible inhibition of CYP activity in HLM with CAW-R61J or control reversible CYP inhibitors.

CYP	Control Inhibitor	Maximal Concentration (μM)	Control IC_{50} (μM)	CAW-R61J IC_{50} (μg/mL)
1A2	α-Naphthoflavone	10	0.010	1500
2B6	Sertraline	100	5.3	>1000
2C8	Montelukast	10	0.082	430
2C9	Sulfaphenazole	25	0.26	330
2C19	Benzylnirvanol	25	0.28	520
2D6	Quinidine	10	0.039	850
3A4/5-M	Ketoconazole	25	0.034	810
3A4/5-T	Ketoconazole	5	0.065	>500

DMD Fast Forward. Published on June 24, 2020 as DOI: 10.1124/dmd.120.090860
This article has not been copyedited and formatted. The final version may differ from this version.

TABLE 9. Time dependent inhibition (TDI) of CYP activity in HLM with CAW-R61J or control TDI CYP inhibitors.

CYP	CAW-R61J			Control Inhibition			
	IC_{50} (µg/mL)			Control Inhibitor	Concentration (µM)	% Inhibition	
	-NADPH	+NADPH	Shift			-NADPH	+NADPH
1A2	>1000	>1000	NA	Furafylline	1	78	88
2B6	NC	NC	NA	ThioTEPA	5	18	80
2C8	NC	>1000	NA	Phenelzine	100	38	74
2C9	NC	560	NA	Tienilic Acid	1	39	77
2C19	>1000	660	NA	Ticlopidine	10	17	47
2D6	>1000	180	NA	Paroxetine	0.5	13	48
3A4/5-M	NC	NC	NA	Azamulin	0.5	23	37
3A4/5-T	NC	NC	NA	Azamulin	0.5	42	57

NC – Not calculated i.e. the non-linear regression in Graph Pad Prism could not calculate a unique constant; NA- not applicable

DMD Fast Forward. Published on June 24, 2020 as DOI: 10.1124/dmd.120.090860
This article has not been copyedited and formatted. The final version may differ from this version.

FIGURES

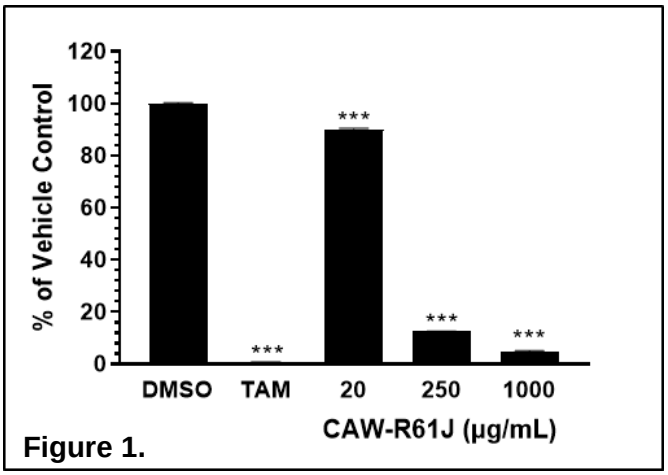

Figure 1.

DMD Fast Forward. Published on June 24, 2020 as DOI: 10.1124/dmd.120.090860
This article has not been copyedited and formatted. The final version may differ from this version.

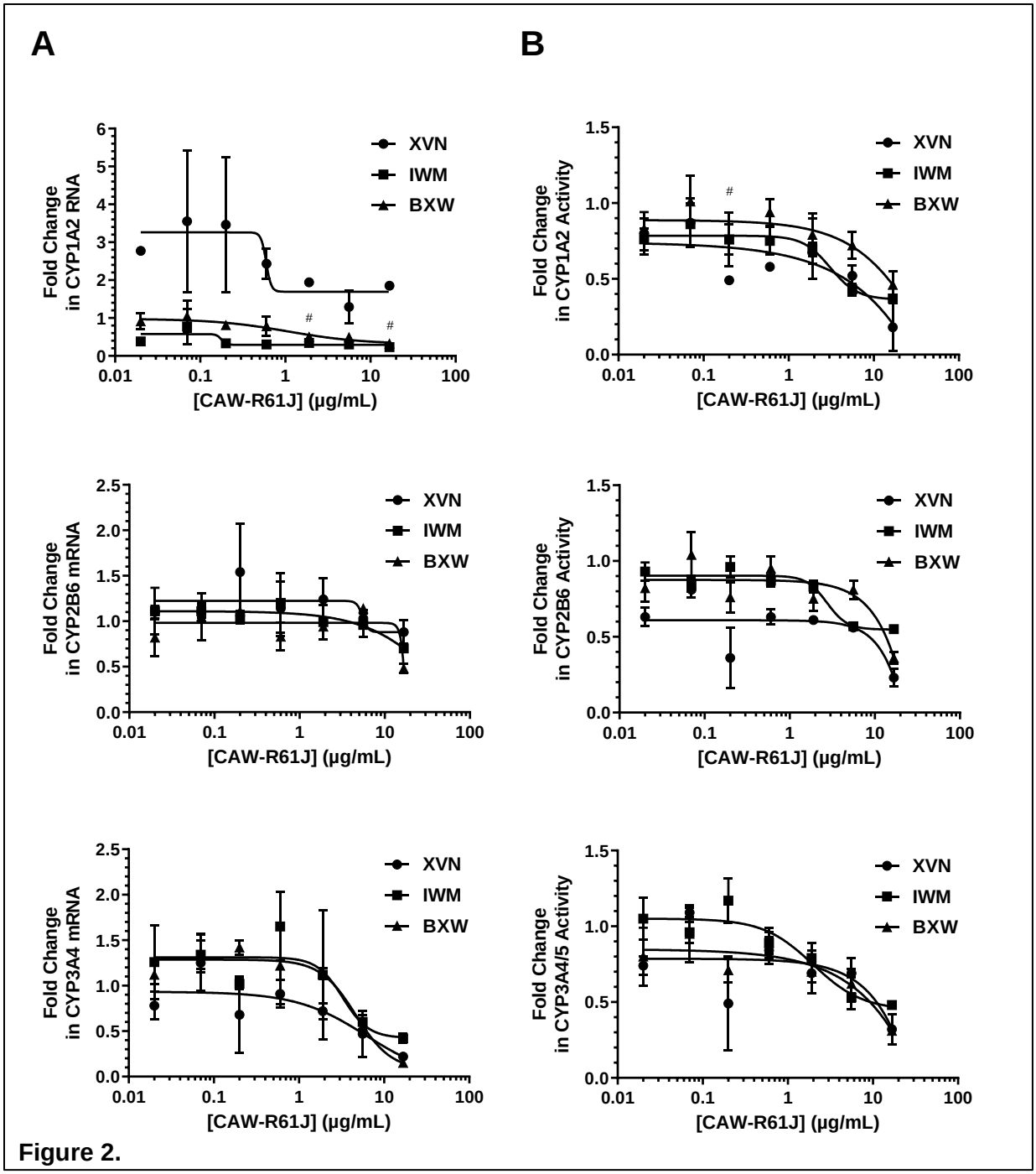

Figure 2.

DMD Fast Forward. Published on June 24, 2020 as DOI: 10.1124/dmd.120.090860
This article has not been copyedited and formatted. The final version may differ from this version.

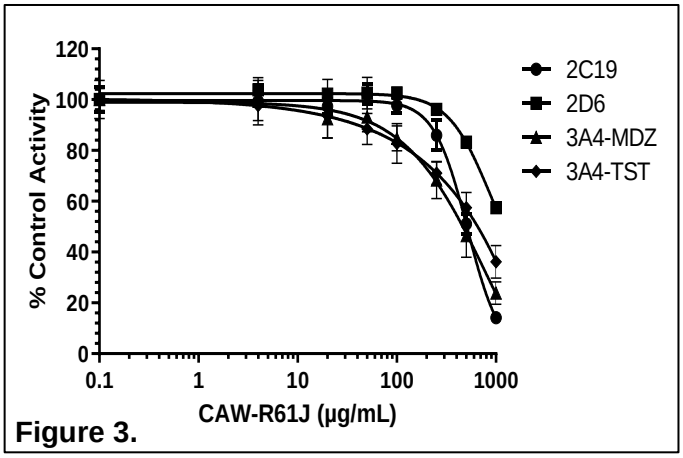

Figure 3.

DMD Fast Forward. Published on June 24, 2020 as DOI: 10.1124/dmd.120.090860
This article has not been copyedited and formatted. The final version may differ from this version.

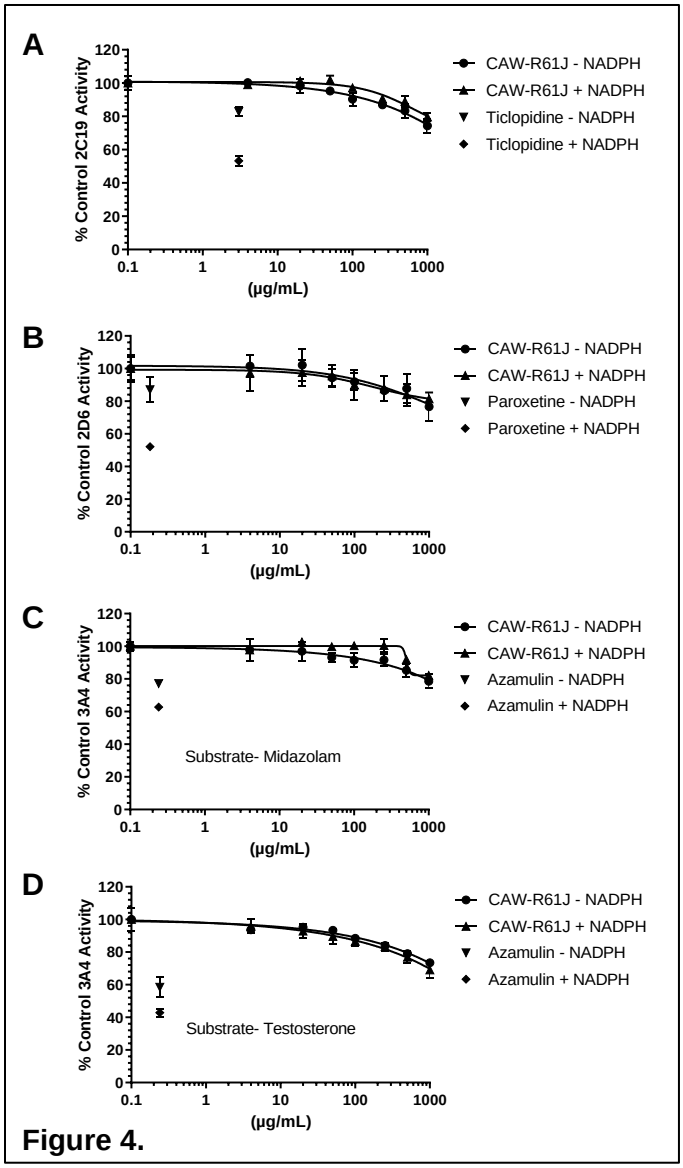

Figure 4.